ACS APPLIED MATERIALS & INTERFACES

RESEARCH ARTICLE

www.acsami.org

Large Dielectric Constant and High Thermal Conductivity in Poly(vinylidene fluoride)/Barium Titanate/Silicon Carbide Three-Phase Nanocomposites

Yong Li,[†] Xingyi Huang,[*,†,‡] Zhiwei Hu,[†] Pingkai Jiang,[*,†] Shengtao Li,[§] and Toshikatsu Tanaka[‡]

[†]Department of Polymer Science and Engineering and Shanghai Key Lab of Electrical Insulation and Thermal Aging, Shanghai Jiao Tong University, Shanghai, China

[‡]IPS Research Center, Waseda University, Kitakyushu, Fukuoka, Japan

[§]State Key Lab of Electrical Insulation and Power Equipment, Xi'an Jiaotong University, Xi'an, China

ABSTRACT: Dielectric polymer composites with high dielectric constants and high thermal conductivity have many potential applications in modern electronic and electrical industry. In this study, three-phase composites comprising poly(vinylidene fluoride) (PVDF), barium titanate (BT) nanoparticles, and β-silicon carbide (β-SiC) whiskers were prepared. The superiority of this method is that, when compared with the two-phase PVDF/BT composites, three-phase composites not only show significantly increased dielectric constants but also have higher thermal conductivity. Our results show that the addition of 17.5 vol % β-SiC whiskers increases the dielectric constants of PVDF/BT nanocomposites from 39 to 325 at 1000 Hz, while the addition of 20.0 vol % β-SiC whiskers increases the thermal conductivity of PVDF/BT nanocomposites from 1.05 to 1.68 W m^{-1} K^{-1} at 25 °C. PVDF/β-SiC composites were also prepared for comparative research. It was found that PVDF/BT/β-SiC composites show much higher dielectric constants in comparison with the PVDF/β-SiC composites within 17.5 vol % β-SiC. The PVDF/β-SiC composites show dielectric constants comparable to those of the three-phase composites only when the β-SiC volume fraction is 20.0%, whereas the dielectric loss of the PVDF/β-SiC composites was much higher than that of the three-phase composites. The frequency dependence of the dielectric property for the composites was investigated by using broad-band (10^{-2}–10^{6} Hz) dielectric spectroscopy.

KEYWORDS: poly(vinylidene fluoride) (PVDF), barium titanate ($BaTiO_3$) nanoparticles, silicon carbide (β-SiC) whiskers, dielectric constant, thermal conductivity

1. INTRODUCTION

Dielectric polymer composites with high dielectric constants have attracted much attention because of their ease of processing and wide range of potential applications.[1−3] To date, two technical routes have been developed to achieve polymer composites with high dielectric constants: the preparation of both percolative composites[2] and ceramic/polymer composites.[4] Percolative systems consisting of insulating polymers and conductive fillers can show very high dielectric constants near the percolation threshold.

So far, numerous percolative composites with high dielectric constants have been reported. Typical conductive components include (i) carbon-based fillers such as carbon black,[5] carbon nanotubes,[6] carbon fiber,[7] graphene,[8,9] graphite platelets,[10] (ii) metal-based fillers such as particles[11] and nanowires,[12] and (iii) conductive polymers such as polyaniline[13,14] and polythiophene.[15] Percolation theory has been widely used to describe dielectric constant enhancement in conductor−insulator composites. According to percolation theory,[11] the effective dielectric constant ε of a conductor−insulator composite is inversely proportional to the difference between the volume content of conductive fillers and the percolation threshold, p_c:

$$\varepsilon = \varepsilon_m (p_c - p)^{-s}, \quad p < p_c \tag{1}$$

where s is the scale constant and ε_m and p are the dielectric constant of the dielectric matrix and the volume fraction of conductive fillers, respectively. According to eq 1, a very high dielectric constant can be achieved if the composites contain an appropriate volume fraction of conductive filler. Although a very high capacitance or dielectric constant can be realized, the conductor−insulator composites cannot withstand a high electric field because of the very high electrical conductivity of the fillers, resulting in some limitations for certain applications. According to the model of Beale and Duxbury,[16] the breakdown strength E_{bre} of conductor-loaded dielectric composites behaves as

$$E_{bre} = \frac{(p_c - p_{conductor})^{\nu}}{\ln L} \tag{2}$$

where L indicates the linear dimension of the composites and $p_{conductor}$ and p_c are the content of the conductive fillers and the percolation threshold, respectively. According to eq 2, one can see that the breakdown strength tends to zero if the conductive filler loading approaches the percolation threshold. It should be noted that several methods have been proposed to increase the breakdown strength of metal-particle-based polymer composites while maintaining the high dielectric constant, for example, using core−shell-structured silver nanoparticles or self-passivated aluminum particles as fillers.[17−20] Although a relatively high short-time breakdown strength is observed in these composites, there

Received: August 5, 2011
Accepted: October 18, 2011
Published: October 18, 2011

is still a lack of data on the long-time performance of these composites. It must be pointed out that, in the high voltage insulation industry, conductive particles are contaminants causing electrical stress enhancement of the insulation and should be removed during production of the insulation.[21]

Another popular strategy used is the incorporation of a high-dielectric-constant ceramic filler such as $BaTiO_3$ into a polymer.[22−33] The advantage of this method is that, although the breakdown strength of the polymer/ceramic composites is generally lower than that of pure polymers, the composites can withstand a relatively high electric field.[34] The increase in the dielectric constant originates from an increase of the electric field in the polymer matrix.[35] Currently, research interest is focused on the fabrication of high-dielectric-constant polymer-based nanocomposites. Poly(vinylidene fluoride) (PVDF)-based polymers, such as poly(vinylidene fluoride-*co*-trifluoroethylene) [PVDF-TrFE], poly(vinylidene fluoride-*co*-hexafluoropropylene) [PVDF-HFP], and poly(vinylidene fluoride-*co*-trifluoroethylene-*co*-chlorotrifluoroethylene) [PVDF-TrFE-CTFE], have been used to prepare high-dielectric-constant composites.[1,25,26,33,36,37] Using this method, however, we can only observe a limited increase of the dielectric constant (by a factor of 10) even at high ceramic filler loading.

Recently, several reports showed that the dielectric constant of a two-phase polymer/ceramic composite can be increased by introducing a third component. It was reported by Prskash and Varma that the dielectric constant of an epoxy composite containing 40.0% $CaCu_3Ti_4O_{12}$ is about 50, and a dielectric constant value of 200 at 100 Hz can be achieved through the addition of 20.0 vol % aluminum nanoparticles to an epoxy composite containing 20.0 vol % $CaCu_3Ti_4O_{12}$.[38] More recently, the work of George and Sebastian showed that the addition of 28.0 vol % silver can increase the dielectric constant of epoxy/ceramic composites from 8 to 142 at 1 MHz.[39] Although the dielectric constants of two-phase polymer/ceramic composites are significantly increased by the addition of a conducting component, the breakdown strengths of three-phase composites are significantly lowered because of the existence of conductive fillers, and thus their applications are limited in many fields.

In this work, three-phase dielectric composites comprising ferroelectric polymer PVDF, barium titanate (BT) nanoparticles, and β-silicon carbide (β-SiC) nanowiskers were fabricated and a large dielectric constant higher than 300 at 1000 Hz was observed. β-SiC was chosen as the third component because β-SiC-based polymer composites can withstand a certain electric field and have been widely used for corona protection of motor stator bars and for electric stress control of medium-voltage cable accessories.[40] It was found that, when compared with two-phase PVDF/BT composites with the same filler loading, three-phase composites not only have significantly increased dielectric constants but also show much higher thermal conductivity. High thermal conductivity and high dielectric constants also suggest that the devices made from three-phase composites are possible with higher packaging densities and enhanced heat dissipation; thereby a property improvement of these devices will be achieved.

2. EXPERIMENTAL SECTION

2.1. Raw Materials. Poly(vinylidene fluoride) (PVDF, FR 401) was purchased from Shanghai 3F New Material Co., Ltd., China. Barium titanate (BT) nanoparticles (100 nm) were obtained from Shandong Sinocera Functional Material Co., Ltd., China. γ-(Aminopropyl)-triethoxysilane (A-1100) was supplied by GE Silicones. β-Silicon carbide (β-SiC) whiskers with an average diameter of 100 nm and an average length of 2 μm were purchased from Xuzhou Hongwu Nanometer Material Co., Ltd. China. Dimethylformamide (DMF) and ethanol were supplied by Sinopharm Chemical Reagent Co., China. All chemicals were used as received.

2.2. Surface Modification of BT Nanoparticles. The surface modification of BT nanoparticles involved several steps: (i) dispersing BT nanoparticles in an ethanol/water solution under sonication, (ii) adding A-1100 to the BT/ethanol/water mixture, (iii) heating to 70 °C and stirring for 2 h, (iv) centrifuging and washing the BT nanoparticles with fresh ethanol, and (v) drying at 80 °C overnight under vacuum.

2.3. Preparation of Composites. The desired amount of PVDF was dissolved in the smallest possible amount of DMF by stirring at 60 °C. At the same time, the desired amounts of BT nanoparticles and β-SiC whiskers were dispersed in DMF under sonication. Then, the suspension was poured into the PVDF solution. The obtained mixture was stirred at 60 °C for 30 min and then at 120 °C for about 4 h to evaporate the majority of DMF. The resulting composite was heated at 140 °C in a vacuum oven to remove the residual solvent. Finally, it was compression-molded at 190 °C for 10 min under a pressure of about 10 MPa. For PVDF with 60.0 vol % BT, 240 °C was used for the sample compression molding. Films with thicknesses of around 500 ± 50 μm were used for measurements. All of the samples were kept in a desiccator before the measurements.

2.4. Characterization. The cryofractured surface of PVDF composites was observed by using a JEOL JEM-7401 field-emission scanning electron microscope. The composite sheets were first broken, and then the fractured surface was sputtered with thin layers of gold to avoid accumulation of charges.

The dielectric properties were measured by using a Solartron SI 1260 impedance analyzer (Advanced Measurement Technology, Inc., Wokingham, U.K.) in the frequency range of 10^{-2}−10^{6} Hz. All of the samples have a layer of gold evaporated on both surfaces to serve as electrodes. The sample is considered to be a plane capacitor and is described by a parallel resistor−capacitor circuit system. The complex dielectric constant (ε^*), complex impedance (Z^*), and electric modulus (M^*) are calculated as follows:

$$\varepsilon^* = \varepsilon' - j\varepsilon'' \tag{3}$$

$$Z^* = Z' - jZ'' = 1/j\omega C_0\varepsilon^* \tag{4}$$

$$M^* = M' + jM'' = 1/\varepsilon^* \tag{5}$$

where ε' and ε'' correspond to the real and imaginary parts of the complex dielectric constant, Z' and Z'' represent the real and imaginary parts of the complex impedance, M' and M'' correspond to the real and imaginary parts of the complex electric modulus, $\omega = 2\pi f$ is the angular frequency, C_0 is the free space capacitance, and $j = (-1)^{1/2}$.

$$\varepsilon' = \frac{-Z''}{\omega C_0(Z'^2 + Z''^2)} \tag{6a}$$

$$\varepsilon'' = \frac{Z'}{\omega C_0(Z'^2 + Z''^2)} \tag{6b}$$

$$M' = \frac{\varepsilon'}{\varepsilon'^2 + \varepsilon''^2} \tag{7a}$$

$$M'' = \frac{\varepsilon''}{\varepsilon'^2 + \varepsilon''^2} \tag{7b}$$

The dielectric loss tangent ($\tan\delta$) is defined as

$$\tan\delta = \frac{\varepsilon''}{\varepsilon'} = \frac{Z'}{Z''} = \frac{M''}{M'} \quad (8)$$

The thermal diffusivity (δ) and specific heat (C) were measured on disk samples by using a LFA447 light flash system (NETZSCH, Selb, Germany) at 25 °C. The bulk density (ρ) of the specimen was measured by water displacement. The thermal conductivity (λ, W m^{-1} K^{-1}) was given by the product of the thermal diffusivity (δ, mm^2 s^{-1}), specific heat (C, J g^{-1} K^{-1}), and bulk density (ρ, g cm^{-3}):

$$\lambda = \delta C \rho \quad (9)$$

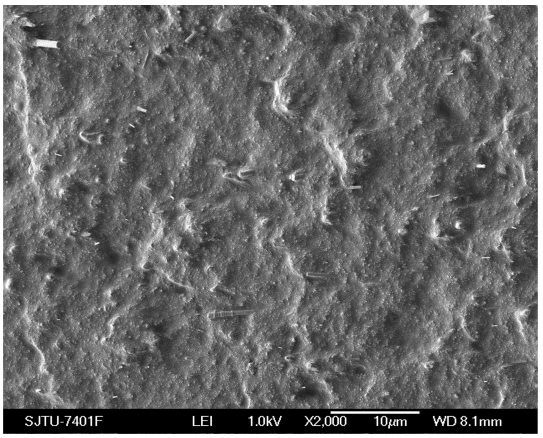

Figure 1. Morphology of the fractured surface of PVDF/BT/β-SiC composites.

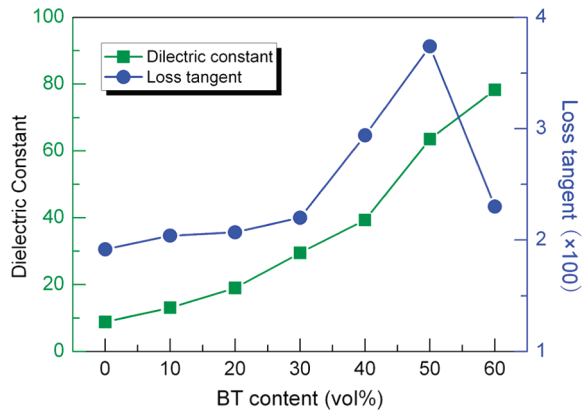

Figure 2. Dielectric constant and loss tangent of PVDF/BT nanocomposites at 1000 Hz and room temperature. The lines are guides for the eyes.

3. RESULTS AND DISCUSSION

3.1. Morphology. Figure 1 shows the cryofractured surface morphology of PVDF/BT/β-SiC composites. This scanning electron microscopy image reveals that the β-SiC whiskers are well dispersed in the PVDF/BT composites. The whiskers are pulled out from the BT-based composites, indicating that the interface between the β-SiC whiskers and PVDF is not strong.

3.2. Dielectric Properties of PVDF/BT Nanocomposites. Figure 2 displays the dielectric constant measured at 1000 Hz as a function of the volume fraction of BT nanoparticles. As expected, the dielectric constant of the composites increases with the BT loading. The dielectric loss tangent of the composites increases as the BT loading increases to 50.0 vol %. When the BT loading is 60.0 vol %, the dielectric loss tangent of the composite shows a decreased value. This phenomenon may be related to the phase inversion. When the BT loading is larger than 50.0 vol %, PVDF becomes the discontinuous phase from the continuous phase, resulting in a decrease in the leak current and thus decreased dielectric loss.

As shown in Figure 2, at 60.0 vol %, BT nanoparticles can provide a dielectric constant of around 80 at 1000 Hz. However, we cannot further increase the BT loading for a higher dielectric constant because the composite with a BT loading larger than 60.0 vol % loses the material processability. In order to further increase the dielectric constant while keeping the filler content, PVDF/BT/β-SiC three-phase composites were prepared, which contained 40.0 vol % BT and not more than 20.0 vol % β-SiC whiskers. Meanwhile, two-phase composites comprising PVDF and β-SiC were also prepared for a comparative research. Figure 3 shows the dependence of the dielectric parameters of PVDF/β-SiC and PVDF/BT/β-SiC composites on the volume fraction of β-SiC at 1000 Hz. As shown in Figure 3, the dielectric constant of PVDF/BT composites increases dramatically after the introduction of β-SiC whiskers. For example, the dielectric constant of the PVDF/BT/β-SiC composite was found to reach its maximum of 325 at a β-SiC loading of 17.5 vol %, about an 8-fold

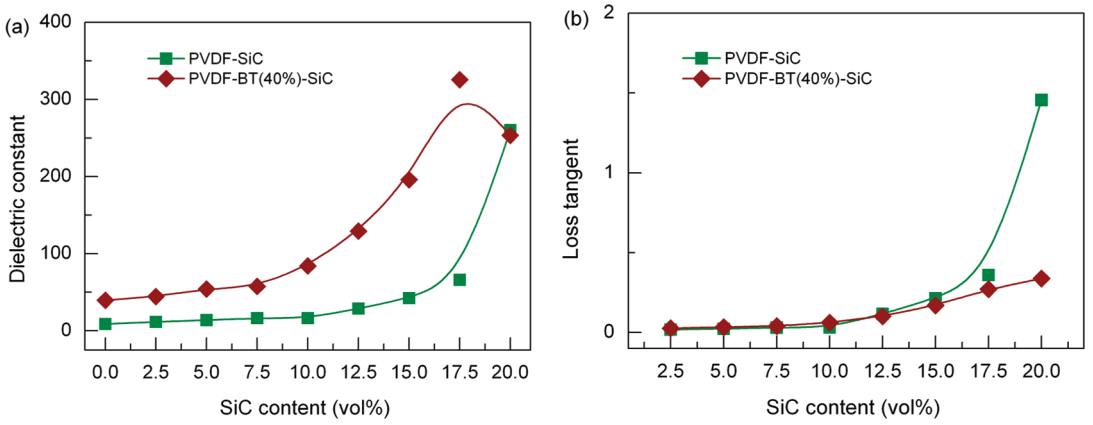

Figure 3. Dielectric parameters of PVDF/β-SiC and PVDF/BT/β-SiC composites at 1000 Hz and room temperature. The lines are guides for the eyes.

increase in the dielectric constant for the PVDF composite with 40.0 vol % BT. As the β-SiC loading is increased further to 20.0 vol %, the dielectric constant of the PVDF/BT/β-SiC composite decreases to 253. This phenomenon has been observed in many polymer/ceramics composite systems and can be generally explained as a consequence of the formation of voids and porosity.[41]

It should be noted from Figure 3 that, at the maximum loading of 20.0 vol %, the PVDF/β-SiC composites also show relatively high dielectric constants (around 260). However, the dielectric loss tangent of the PVDF/β-SiC composites is much higher than that of three-phase composites. For instance, when the β-SiC whisker loading is 20.0 vol %, the values of the loss tangent of PVDF/β-SiC and PVDF/BT/β-SiC are 1.46 and 0.34, respectively. On the other hand, a high dielectric constant can only be observed in the sample with the maximum β-SiC loading of 20.0 vol %. These results show the superiority of three-phase composites for fulfilling low loss and high dielectric constant. The decrease of the dielectric loss in three-phase composites is due to the isolation effect of BT nanoparticles on the β-SiC whiskers.

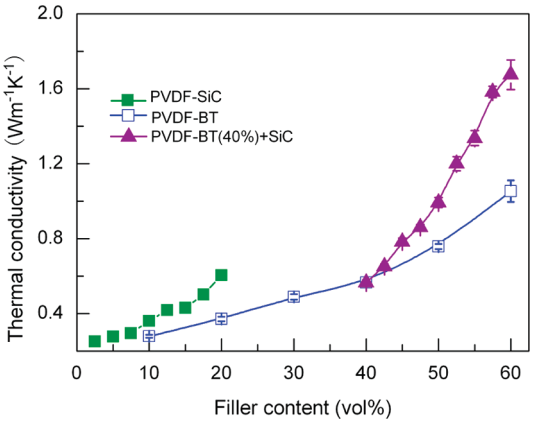

Figure 4. Thermal conductivity of PVDF/BT, PVDF/β-SiC, and PVDF/BT/β-SiC composites at 25 °C. The lines are guides for the eyes.

3.3. Thermal Conductivity of the PVDF/BT and PVDF/BT/β-SiC Composites. The thermal conductivity of the composites is given in Figure 4. It appears that all of the composites show an increase in the thermal conductivity with increasing filler loading. Clearly, the thermal conductivity of the composites filled with β-SiC whiskers is much higher than that of the PVDF/BT composites. For instance, when the filler loading is 20.0 vol %, the thermal conductivity values of PVDF/BT and PVDF/β-SiC are 0.37 and 0.60 W m^{-1} K^{-1}, respectively. On the other hand, the PVDF/BT/β-SiC composites have much higher thermal conductivity in comparison with the PVDF/BT composites if the total filler loading is the same. According to Figure 4, the sample with 60.0 vol % BT and the sample with 40.0 vol % BT plus 20.0 vol % β-SiC show thermal conductivity values of 1.05 and 1.67 W m^{-1} K^{-1}, respectively. There are two possible reasons for the higher thermal conductivity of the composites containing β-SiC whiskers.[42] The first should be due to the higher intrinsic thermal conductivity of β-SiC in comparison with BT. According to the reported values, β-SiC and BT have thermal conductivity values of 85 and 6.2 W m^{-1} K^{-1}, respectively.[42] The aspect ratio of the fillers has been known as another factor influencing the thermal conductivity of composites. The β-SiC filler used in this work has a high aspect ratio and thus can form more conductive pathways, leading to a higher thermal transfer rate in comparison with BT.

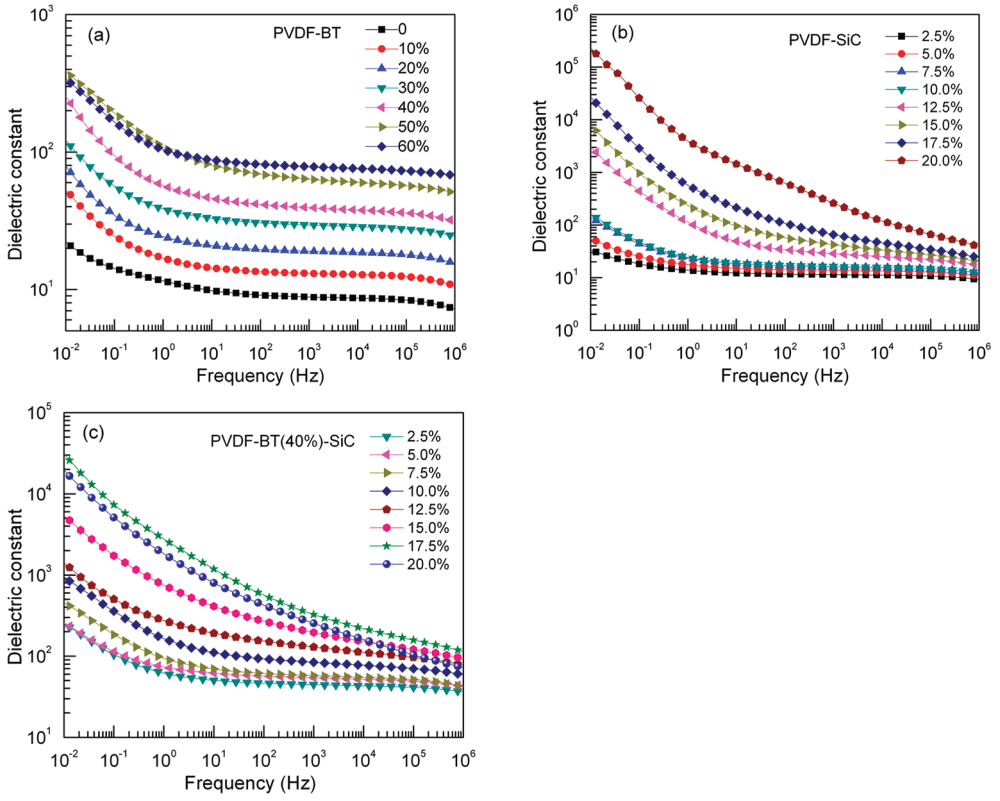

Figure 5. Frequency dependence of the real part of the dielectric constant for PVDF/BT, PVDF/β-SiC, and PVDF/BT/β-SiC composites. The numbers in the legend indicate the volume fraction of BT (a) and β-SiC (b and c).

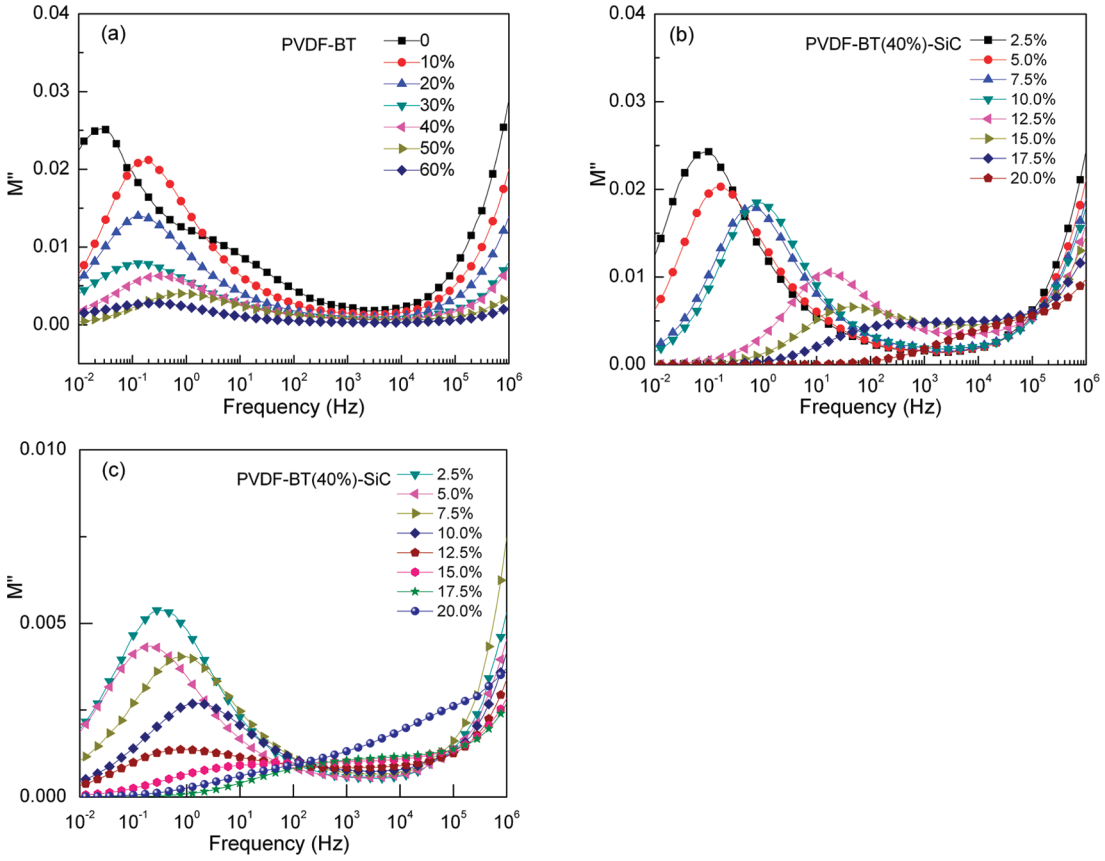

Figure 6. Frequency dependence of the imaginary part of the electric modulus for PVDF/BT, PVDF/β-SiC, and PVDF/BT/β-SiC composites. The numbers in the legend indicate the volume fraction of BT (a) and β-SiC (b and c).

3.4. Frequency Dependence of the Dielectric Properties. Figure 5 shows the frequency dependence of the dielectric constants of PVDF/BT, PVDF/β-SiC, and PVDF/BT/SiC composites for different filler loadings at room temperature. We can see that (i) in the case of PVDF/BT composites, the dielectric constant shows a rapid decrease with the frequency at the low-frequency range and becomes almost constant at high frequencies, (ii) when the SiC filler is low, the dielectric constants of the PVDF/β-SiC and PVDF/BT/β-SiC composites show frequency dependence behavior similar to that of PVDF/BT composites; (iii) the dielectric constants of the PVDF/β-SiC and PVDF/BT/β-SiC composites with high β-SiC loading decrease with the frequency over the whole frequency range. The decrease of the dielectric constant with the frequency can be explained by the interfacial polarization mechanism. Because of the large electrical conductivity difference between the polymer matrix and the fillers, charge carriers from the electrode and/or the impurities of composites can migrate and accumulate at the interface between the filler and polymer if an electric field is applied on the sample.[43] The migration and accumulation process of the charge carriers can cause large polarization and a very high dielectric constant.

Interfacial polarization in PVDF/BT composites decreases with increasing frequency and then reaches a constant at a certain frequency because of the following facts: (i) the BT nanoparticles used were surface-treated by a silane coupling agent and some unbounded impurities might be removed during this process, resulting in a decrease in the number of charge carriers; (ii) the charge carriers in the composites with surface-treated BT become bounded; therefore, their migration and accumulation process needs a relatively long time; (iii) both PVDF and BT are dielectric materials; the electrical conductivity difference between them is relatively low.

In order to show more information about the interfacial polarization of the composites, the dielectric modulus formalism is given in Figure 6. The advantages of the electric modulus formalism to interpret bulk relaxation properties over others are their independence of electrode nature and contact, space charge injection, and absorbed impurity conduction, which appear to obscure relaxation in the dielectric spectrum formalism.[44]

The imaginary part (M'') of the electric modulus takes the form of loss curves, allowing us to interpret the relaxation phenomena within the bulk of materials. Up to now, the electric modulus formalism has been utilized to investigate the dipole relaxation process, interfacial polarization, and long-range conduction process within the bulk of materials.[44,45] As shown in Figure 6, a relaxation process associated with interfacial polarization can be clearly observed in the M'' curves of the three types of composites. For the PVDF/BT composites (Figure 6a), we can see that the relaxation strength decreases with the BT loading, whereas the relaxation peak frequency and relaxation range are almost not changed. According to Figure 6a, the loss peak appears at the low-frequency range for each composite, indicating that the interfacial polarization only appears at low frequencies in PVDF/BT composites. Both PVDF and BT are high-resistivity materials at room temperature, and thus the charge

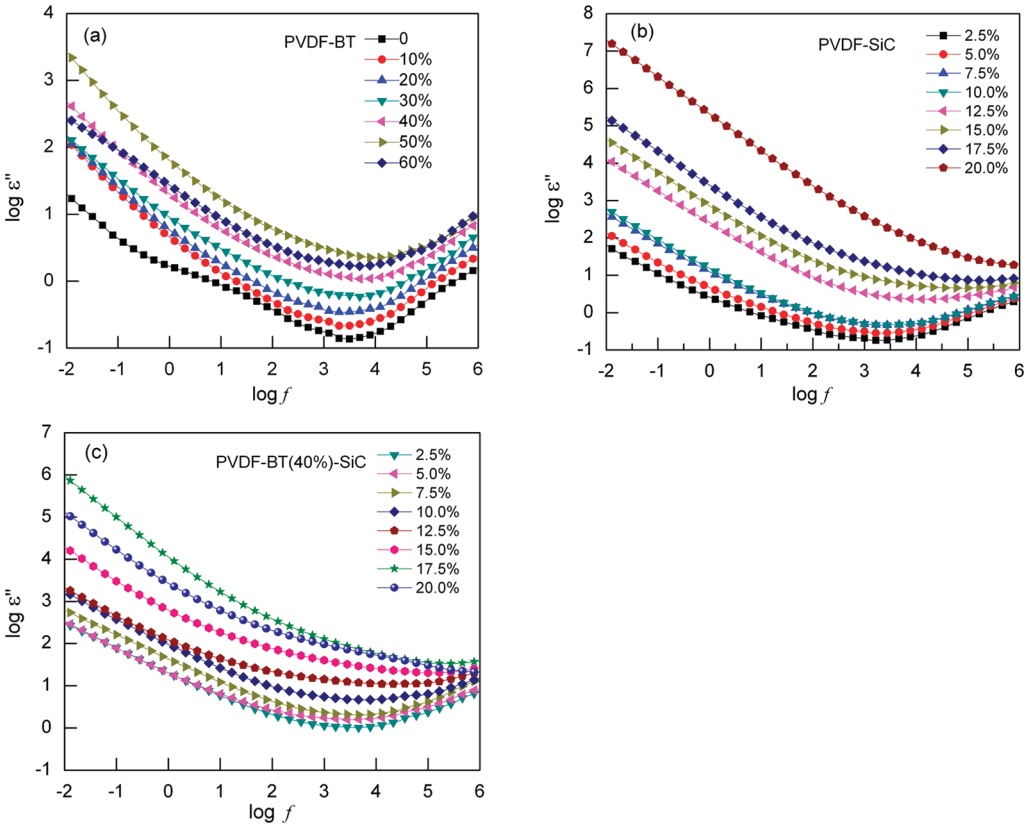

Figure 7. Frequency dependence of the imaginary part of the dielectric constant for PVDF/BT, PVDF/β-SiC, and PVDF/BT/β-SiC composites. The numbers in the legend indicate the volume fraction of BT (a) and β-SiC (b and c).

carriers have a low mobility within the bulk of PVDF/BT nanocomposites. In such a case, there should be a considerable time interval required for charge carriers to reach an interface; namely, interfacial polarization takes long time to be established, so interfacial polarization appears at low frequencies.[46]

The M'' curve of the pure PVDF shows two relaxation peaks at low frequencies. The peak at 1 Hz is attributed to α_c relaxation, which is associated with the molecular motion in the crystalline region of PVDF.[47] Another relaxation peak at about 0.03 Hz is attributed to interfacial polarization, which is due to the charge accumulation on the boundary between the lamellar crystal and interlamellar amorphous region. After introduction of the BT nanoparticles, the charge carriers also accumulate on the surface of BT, which is the reason for the shift of the interfacial polarization relaxation peaks of PVDF/BT nanocomposites to higher frequencies. The reason for the absence of the α_c peak in PVDF composites is not yet clear, and it is supposed that the BT nanoparticles result in a suppressive effect on the molecular motion in the crystalline region of PVDF.

For composites with β-SiC whiskers, the large difference of the electrical conductivity between the filler and polymer cause a strong interfacial polarization, and thus the PVDF/β-SiC and PVDF/BT/β-SiC composites can have very high values of the dielectric constant at low frequencies. As the β-SiC loading becomes higher, the β-SiC whiskers come into contact with each other, which can result in long-range charge carrier migration. In such a case, not only is the dielectric constant high but also its value decreases with the frequency at a wide frequency range. Such an explanation can be confirmed by the M'' curves of the PVDF/β-SiC and PVDF/BT/β-SiC composites. As shown in parts b and c of Figure 6, the interfacial polarization relaxation peaks become broader and move to high frequencies with increasing β-SiC loading.

The intrinsic immobilized charge carriers can move freely under an electric field and then accumulate on the interface between the insulating polymers and the fillers because of the conductivity and dielectric constant difference between them, resulting in interfacial polarization. As the fraction of β-SiC whisker increases, the composites show increases in the β-SiC cluster size and/or number, which leads to a higher possibility for the charge carriers to accumulate on the interface between β-SiC and PVDF, resulting in a short relaxation time. Therefore, the relaxation process in PVDF/β-SiC composites shifts to higher frequencies. For three-phase composites with lower β-SiC loading, however, the shift of the interfacial polarization relaxation peaks is to be diminished because of the isolation effect of BT nanoparticles on β-SiC whiskers.

The dielectric loss, ε'', is defined as the product of the real part of the dielectric constant and dielectric loss tangent, describing the energy dissipation in a dielectric material through conduction (transport-related loss), slow polarization currents (dipolar loss), and other dissipative phenomena (interfacial polarization contribution).[29,34,44,48]

For a composite, ε'' can be expressed as

$$\varepsilon'' = \varepsilon_{dc}'' + \varepsilon_{MW}'' + \varepsilon_{D}'' \quad (10)$$

where ε_{dc}'' and ε_{MW}'' are related to conduction and interfacial polarization, respectively, and ε_{D}'' is the dipole loss factor.

The conduction loss factor ε_{dc}'' is given by

$$\varepsilon_{dc}'' = \frac{\sigma_{dc}}{2\pi f} \quad (11)$$

where σ_{dc} and f represent the direct current conductivity and frequency, respectively. According to eq 11, log ε'' versus log f represents a straight line.

Figure 7 shows the frequency dependence of ε'' for PVDF/BT, PVDF/β-SiC, and PVDF/BT/β-SiC composites. It appears that ε'' decreases with the frequency at low frequencies and increases with the frequency at high frequencies. It is generally believed that the high-frequency process is mainly associated with dipolar relaxation, whereas at lower frequencies, the contributions of interfacial polarization and conductivity are significant.[43,46] The plots of log ε'' versus log f for the PVDF/BT composites do not show strict linear relationships at low frequencies, indicating that the conduction loss is not dominant at low frequencies. The log ε''−log f plots of PVDF/β-SiC and PVDF/BT/β-SiC composites, in particular the composites with higher SiC loading, show strict linear slopes at low frequencies, suggesting that the conduction loss is dominant in the low-frequency range. It should be noted from Figure 7 that the plots of log ε'' versus log f for PVDF/β-SiC show linear relationships at a wider range of frequency when compared with the PVDF/BT/β-SiC composites with the same β-SiC loading. As discussed earlier, this result means that the BT nanoparticles show an isolation effect on the β-SiC whiskers in the composites.

4. CONCLUSIONS

Three-phase PVDF/BT/SiC composites were prepared, which have higher dielectric constants and higher thermal conductivity in comparison with PVDF/BT composites with the same filler loading. The three-phase composite with 17.5 vol % β-SiC whiskers has a dielectric constant of 325 at 1000 Hz. On the other hand, the addition of 20.0 vol % β-SiC whiskers increases the thermal conductivity of PVDF/BT nanocomposites from 1.05 to 1.68 W m^{-1} K^{-1} at 25 °C.

It was also found that, when the β-SiC volume fraction is 20.0%, PVDF/β-SiC composites can have dielectric constants comparable with those of three-phase composites, whereas the dielectric loss of PVDF/β-SiC composites is much higher than that of three-phase composites.

When compared with PVDF/BT composites, PVDF/β-SiC and PVDF/BT/β-SiC composites show a stronger frequency dependence of dielectric parameters. The interfacial polarization mechanism can be used to explain the observed dielectric phenomenon.

AUTHOR INFORMATION

Corresponding Author

*E-mail: xyhuang@sjtu.edu.cn (X.Y.H.), pkjiang@sjtu.edu.cn (P.K.J.).

ACKNOWLEDGMENT

The authors gratefully acknowledge support from the National Science Foundation of China (Grant 51107081), the Research Fund for the Doctoral Program of Higher Education (Grant 20100073120038), the National Undergraduate Innovative Test Program (ITP, PP2067, and PP3070), and the Shanghai Leading Academic Discipline Project (Grant B202). The present work was also supported by State Key Laboratory of Electrical Insulation and Power Equipment (Grant EIPE11206).

REFERENCES

(1) Bai, Y.; Cheng, Z. Y.; Bharti, V.; Xu, H. S.; Zhang, Q. M. *Appl. Phys. Lett.* **2000**, *76*, 3804.
(2) Nan, C. W.; Shen, Y.; Ma, J. *Annu. Rev. Mater. Res.* **2010**, *40*, 131.
(3) Zhang, Q. M.; Li, H. F.; Poh, M.; Xia, F.; Cheng, Z. Y.; Xu, H. S.; Huang, C. *Nature* **2002**, *419*, 284.
(4) Lu, J. X.; Wong, C. P. *IEEE Trans. Dielectr. Electr. Insul.* **2008**, *15*, 1322.
(5) Nelson, P. N.; Hervig, H. C. *IEEE Trans. Power Appar. Syst.* **1984**, *103*, 3211.
(6) Wang, L.; Dang, Z. M. *Appl. Phys. Lett.* **2005**, *87*, 042903.
(7) Sui, G.; Jana, S.; Zhong, W. H.; Fuqua, M. A.; Ulven, C. A. *Acta Mater.* **2008**, *56*, 2381.
(8) Yu, J. H.; Huang, X. Y.; Wu, C.; Jiang, P. K. *IEEE Trans. Dielectr. Electr. Insul.* **2011**, *18*, 478.
(9) Wu, C.; Huang, X. Y.; Xie, L. Y.; Wu, X. F.; Yu, J. H.; Jiang, P. K. *J. Mater. Chem.* **2011**, http://dx.doi.org/10.1039/C1JM12903A.
(10) He, F.; Lau, S.; Chan, H. L.; Fan, J. T. *Adv. Mater.* **2009**, *21*, 710.
(11) Xu, J. W.; Wong, C. P. *Appl. Phys. Lett.* **2005**, *87*, 082907.
(12) Zheng, W.; Lu, X. F.; Wang, W.; Wang, Z. J.; Song, M. X.; Wang, Y.; Wang, C. *Phys. Status Solidi A* **2010**, *207*, 1870.
(13) Huang, C.; Zhang, Q. M.; Su, J. *Appl. Phys. Lett.* **2003**, *82*, 3502.
(14) Yuan, J. K.; Dang, Z. M.; Yao, S. H.; Zha, J. W.; Zhou, T.; Li, S. T.; Bai, J. B. *J. Mater. Chem.* **2010**, *20*, 2441.
(15) Carpi, F.; Gallone, G.; Galantini, F.; De Rossi, D. *Adv. Funct. Mater.* **2008**, *18*, 235.
(16) Beale, P. D.; Duxbury, P. M. *Phys. Rev. B* **1988**, *37*, 2785.
(17) Huang, X. Y.; Jiang, P. K.; Kim, C. N.; Ke, Q. Q.; Wang, G. L. *Compos. Sci. Technol.* **2008**, *68*, 2134.
(18) Huang, X. Y.; Jiang, P. K.; Kim, C. U. *J. Appl. Phys.* **2007**, *102*, 124103.
(19) Huang, X. Y.; Ma, Z. S.; Wang, Y. Q.; Jiang, P. K.; Yin, Y.; Li, Z. *J. Appl. Polym. Sci.* **2009**, *113*, 3577.
(20) Shen, Y.; Lin, Y. H.; Nan, C. W. *Adv. Funct. Mater.* **2007**, *17*, 2405.
(21) Bostrom, J. O.; Marsden, E.; Hampton, R. N.; Nilsson, U.; Lennartsson, H. *IEEE Electr. Insul. M* **2003**, *19* (4), 6.
(22) Dang, Z. M.; Zheng, Y.; Xu, H. P. *J. Appl. Polym. Sci.* **2008**, *110*, 3473.
(23) Guo, N.; DiBenedetto, S. A.; Tewari, P.; Lanagan, M. T.; Ratner, M. A.; Marks, T. J. *Chem. Mater.* **2010**, *22*, 1567.
(24) Jung, H. M.; Kang, J. H.; Yang, S. Y.; Won, J. C.; Kim, Y. S. *Chem. Mater.* **2010**, *22*, 450.
(25) Kim, P.; Doss, N. M.; Tillotson, J. P.; Hotchkiss, P. J.; Pan, M. J.; Marder, S. R.; Li, J. Y.; Calame, J. P.; Perry, J. W. *ACS Nano* **2009**, *3*, 2581.
(26) Li, J. J.; Claude, J.; Norena-Franco, L. E.; Il Seok, S.; Wang, Q. *Chem. Mater.* **2008**, *20*, 6304.
(27) Popielarz, R.; Chiang, C. K.; Nozaki, R.; Obrzut, J. *Macromolecules* **2001**, *34*, 5910.
(28) Wang, G. *ACS Appl. Mater. Interface* **2010**, *2*, 1290.
(29) Xie, L. Y.; Huang, X. Y.; Wu, C.; Jiang, P. K. *J. Mater. Chem.* **2011**, *21*, 5897.
(30) Huang, X. Y.; Xie, L. Y.; Hu, Z. W.; Jiang, P. K. *IEEE Trans. Dielectr. Electr. Insul.* **2011**, *18*, 375.
(31) Arbatti, M.; Shan, X. B.; Cheng, Z. Y. *Adv. Mater.* **2007**, *19*, 1369.
(32) Barber, P.; Pellechia, P. J.; Ploehn, H. J.; zur Loye, H. C. *ACS Appl. Mater. Interface* **2010**, *2*, 2553.
(33) Kim, P.; Jones, S. C.; Hotchkiss, P. J.; Haddock, J. N.; Kippelen, B.; Marder, S. R.; Perry, J. W. *Adv. Mater.* **2007**, *19*, 1001.
(34) Huang, X. Y.; Xie, L. Y.; Jiang, P. K.; Wang, G. L.; Liu, F. *J. Phys. D: Appl. Phys.* **2009**, *42*, 245407.

(35) An, L.; Boggs, S. A.; Callame, J. P. *IEEE Electr. Insul. M* **2008**, *24* (3), 5.
(36) Li, J. J.; Seok, S. I.; Chu, B. J.; Dogan, F.; Zhang, Q. M.; Wang, Q. *Adv. Mater.* **2009**, *21*, 217.
(37) Chu, B. J.; Lin, M. R.; Neese, B.; Zhou, X.; Chen, Q.; Zhang, Q. M. *Appl. Phys. Lett.* **2007**, *91*, 122909.
(38) Prakash, B. S.; Varma, K. B. R. *Compos. Sci. Technol.* **2007**, *67*, 2363.
(39) George, S.; Sebastian, M. T. *Compos. Sci. Technol.* **2009**, *69*, 1298.
(40) Donzel, L.; Greuter, F.; Christen, T. *IEEE Electr. Insul. M* **2011**, *27* (2), 18.
(41) Calame, J. P. *J. Appl. Phys.* **2006**, *99*, 084101.
(42) Huang, X. Y.; Jiang, P. K.; Tanaka, T. *IEEE Electr. Insul. M* **2011**, *27* (4), 8.
(43) Dalkin, T. W. *IEEE Electr. Insul. M* **2006**, *22* (5), 11.
(44) Soares, B. G.; Leyva, M. E.; Barra, G. M. O.; Khastgir, D. *Eur. Polym. J.* **2006**, *42*, 676.
(45) Gerhardt, R. *J. Phys. Chem. Solids* **1994**, *55*, 1491.
(46) Moliton, A. *Applied Electromagnetism and Materials*; Springer: New York, 2007; Chapter 3.
(47) Cebe, P.; Yu, L. *J. Polym. Sci., B: Polym. Phys.* **2009**, *47*, 2520.
(48) Fattoum, A.; Gmati, F.; Bohli, N.; Arous, M.; Mohamed, A. B. *J. Phys. D: Appl. Phys.* **2008**, *41*, 095407.